Fourier-transform spectroscopy of NH: the $c\,^1\Pi$–$a\,^1\Delta$ transition

R. S. Ram and P. F. Bernath

Department of Chemistry, University of Arizona, Tucson, Arizona 85721

Received February 18, 1986; accepted May 28, 1986

The high-resolution Fourier-transform emission spectrum of the $c\,^1\Pi$–$a\,^1\Delta$ transition of NH was recorded and analyzed. Improved line positions and molecular constants were determined from the 1–0, 0–0, and 0–1 vibrational bands. In addition to the rotational constants, lambda-doubling parameters for both the $c\,^1\Pi$ and $a\,^1\Delta$ states were extracted from the line positions.

INTRODUCTION

The NH molecule is, along with CH and OH, one of the most studied free radicals. The major reason for this interest is the wide variety of environments—from flames[1] to stellar atmospheres[2]—in which NH can be found. During our recent reanalysis of the $A\,^3\Pi$–$X\,^3\Sigma^-$ transition of NH,[3] we also detected the $c\,^1\Pi$–$a\,^1\Delta$ system of NH. In this paper we report on the 0–0, 0–1, and 1–0 vibrational bands of the c–a transition. The high-quality Fourier-transform data provide some improvement in molecular constants, including extraction of the lambda doubling in the $a\,^1\Delta$ state.

The NH molecule was first observed by Eder[4] in 1893 through the $A\,^3\Pi$–$X\,^3\Sigma^-$ transition near 3360 Å. The $c\,^1\Pi$–$a\,^1\Delta$ transition near 3240 Å was first observed in the 1930's by three groups at about the same time: Nakamura and Shidei,[5] Dieke and Blue,[6] and Pearse.[7] Hanson *et al.*[8] have studied the corresponding ND spectrum, as have Cheung *et al.*[9] More recently, Ramsay and Sarre[10] have analyzed the 0–1 band. The hyperfine and lambda-doubling parameters of the $c\,^1\Pi$–$a\,^1\Delta$ were observed in a laser experiment on a molecular beam by Ubachs *et al.*[11]

A number of transitions connecting to either $c\,^1\Pi$ or $a\,^1\Delta$, such as $d\,^1\Sigma^+$–$c\,^1\Pi$ (Refs. 12 and 13) and $c\,^1\Pi$–$b\,^1\Sigma^+$,[14] have been observed. The singlet and triplet manifolds were first connected through detection of the $b\,^1\Sigma^+$–$X\,^3\Sigma^-$ transition by Masanet *et al.*[15] The most accurate measurements of this transition were made at high resolution by Cossart.[16] The combination of Cossart's lines[16] with data from Ref. 14 and the c–a lines obtained in this work result in an $a\,^1\Delta$ (v = 0, J = 2)–$X\,^3\Sigma^-$ (v = 0, J = 1, N = 0) separation of 12 688.38(10) cm^{-1}.

The direct $a\,^1\Delta$–$X\,^3\Sigma^-$ transition has also been found.[17] Hall *et al.*[18] detected the fundamental infrared vibration–rotation transition of the long-lived $a\,^1\Delta$ state. Recently Leopold *et al.*[19] observed the far-infrared laser magnetic resonance spectrum of NH and ND in the metastable $a\,^1\Delta$ state.

The NH molecule is produced by electron bombardment or photodissociation of a wide variety of molecules, including NH_3, N_2H_4, CH_3NH_2, NH_3, and HNCO.[20–23] These experiments allow the lifetimes[21,22] of excited states of NH to be determined and provide, in addition, fundamental information about electron and photon dissociation processes. For instance, Alberti and Douglas[23] found that vacuum-ultravolet photodissociation of NH_3 produced an anomalous population distribution in the NH product. By monitoring the $c\,^1\Pi$–$a\,^1\Delta$ fluorescence, they found that the two lambda-doubling components of the $c\,^1\Pi$ state are unequally populated.

EXPERIMENT

The experimental details are provided in our paper on $A\,^3\Pi$–$X\,^3\Sigma^-$.[3] Briefly, the $c\,^1\Pi$–$a\,^1\Delta$ emission of NH was excited in a water-cooled copper hollow-cathode discharge lamp operated at 440-mA current. A continuous flow of 4.5 Torr of helium, 0.12 Torr of nitrogen, and 0.04 Torr of hydrogen provided a strong NH signal. The molecular emission was recorded with the Fourier-transform spectrometer associated with the McMath solar telescope of the National Solar Observatory[24] at Kitt Peak. The spectrum had an unapodized resolution of 0.042 cm^{-1} and was calibrated by using helium atomic lines present in the discharge.

RESULTS

The spectral region 24 500 to 33 500 cm^{-1} has structure that is due to two electronic transitions of NH, namely, $A\,^3\Pi$–$X\,^3\Sigma^-$ and $c\,^1\Pi$–$a\,^1\Delta$. The structure of the bands of the $A\,^3\Pi_i$–$X\,^3\Sigma^-$ transition is strong compared with the structure of the c–a transition and appears with a signal-to-noise ratio of >1000. The structure of the 0–0, 1–0, and 0–1 bands of the c–a system was easily identified owing to the characteristic splitting of each line into two lambda-doubling components. A part of the spectrum of the 0–0 band of this system (near the R head) is given in Fig. 1. The 0–0 band of this system is about five times stronger than the 0–1 band and ten times stronger than the 1–0 band. The 1–1 band is also present, but most of the rotational lines are overlapped by the strong 0–0 band of the A–X system. Therefore this band was not included in the present study. The spectrum was measured by using a computer program called DECOMP developed at the National Solar Observatory. All lines were fitted by a nonlinear least-squares procedure to Voigt line-

0740-3224/86/091170-05$02.00

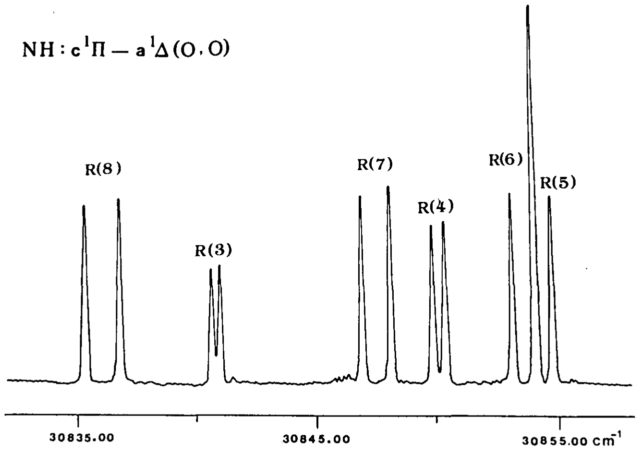

Fig. 1. A portion of the emission spectrum of the $c\,^1\Pi$–$a\,^1\Delta$ 0–0 band. Lambda doubling splits each line into two components (e and f). The band head occurs near 30 855 cm^{-1} at $R(5)$.

shape functions. The estimated precision of measurements for strong, unblended lines of the 0–0 band is of the order of ± 0.001 cm^{-1}, consistent with a line width of about 0.20 cm^{-1} and a signal-to-noise ratio of about 200. For the weaker 1–0 and 0–1 bands, which are frequently obscured by the spectrum of N_2^+ lying in the same spectral region, the precision of measurements is estimated to be ± 0.005 cm^{-1}. The absolute accuracy of the overall frequency calibration[3] is estimated to be ± 0.003 cm^{-1}. Our line-position measurements are systematically 0.0051(31) cm^{-1} higher than those of Ubachs *et al.*[11] Their absolute calibration using iodine may be slightly more secure than ours, which is based on a single helium line.[3]

We have observed the rotational structure up to $J' = 18$ and $J' = 11$ in the bands involving $v = 0$ and $v = 1$ of the $c\,^1\Pi$ state. The study of the $d\,^1\Sigma^+$–$c\,^1\Pi$ transition of this molecule by Graham and Lew[12] clearly established that the $c\,^1\Pi$ state is predissociated beyond $J = 22$ and $J = 15$ in the $v = 0$ and $v = 1$ levels of the $c\,^1\Pi$ state. We were unable to observe the structure up to the point of strong predissociation because of an inadequate signal-to-noise ratio. However, the intensity of the lines decreased much faster than predicted on the basis of a Boltzmann population distribution. A broadening was observed for the lines involving higher J's. For example, the widths of the $Q_{ef}(3)$, $Q_{ef}(10)$, and $Q_{ef}(18)$ lines of the 0–0 band are 0.194, 0.198 and 0.243, respectively, and those of the 1–0 band for the $Q_{ef}(4)$, $Q_{ef}(7)$, and $Q_{ef}(9)$ lines are 0.240, 0.255 and 0.268 cm^{-1}, respectively. The levels affected by predissociation[22] show the broadening most noticeably. Application of the uncertainty principle to the state with the shortest observed lifetime of 41.7 nsec (Ref. 22) for $J' = 9$, $v = 1$ of the $c\,^1\Pi$ state predicts a broadening of only 4 MHz (0.00013 cm^{-1}), much too small to account for the observed increase in broadening.

A plausible explanation is that the high J' (and $v' = 1$) levels, which have emission intensities reduced by predissociation, are highly pressure sensitive. A similar effect was observed for the $A\,^3\Pi$–$X\,^3\Sigma^-$ transition.[3]

The wave numbers of the observed rotational lines of the 0–0, 1–0, and 0–1 bands are given in Tables 1, 2, and 3, respectively, where the branches are labeled according to the e and f parities[25] of the initial and final states.

Table 1. Vacuum Wave Numbers (in cm^{-1}) for the Lines of the 0–0 Band of $c\,^1\Pi$–$a\,^1\Delta$ System of NH[a]

J	R_{ee}	R_{ff}	Q_{ef}	Q_{fe}	P_{ee}	P_{ff}
2	30826.7207(13)	30826.5245(51)	30741.9759(2)	30741.8684(−72)	30685.3962(63)	30685.3552(−13)
3	30840.9634(−6)	30840.6314(1)	30728.2204(−40)	30728.0207(−37)	30643.4834(27)	30643.3778(−28)
4	30850.3427(−7)	30849.8447(−8)	30709.8244(1)	30709.4917(0)	30597.0789(−59)	30596.8794(−54)
5	30854.7459(−7)	30854.0475(−4)	30686.7185(−4)	30686.2205(−7)	30546.1980(−21)	30545.8663(−10)
6	30854.0475(7)	30853.1195(−31)	30658.8357(−7)	30658.1405(−11)	30490.8100(7)	30490.3100(−11)
7	30848.0994(−9)	30846.9154(−8)	30626.0889(0)	30625.1650(−5)	30430.8795(1)	30430.1797(−41)
8	30836.7449(−4)	30835.2713(6)	30588.3717(7)	30587.1932(50)	30366.3639(29)	30365.4347(−16)
9	30819.8001(3)	30818.0056(7)	30545.5601(13)	30544.0879(16)	30297.1907(40)	30296.0034(16)
10	30797.0590(−2)	30794.9166(18)	30497.5092(18)	30495.7181(23)	30223.2716(19)	30221.7958(18)
11	30768.2919(−13)	30765.7706(−1)	30444.0506(22)	30441.9039(−49)	30144.5042(29)	30142.7093(44)
12	30733.2395(−24)	30730.3131(−3)	30384.9892(23)	30382.4719(7)	30060.7512(24)	30058.6053(29)
13	30691.6085(−26)	30688.2493(−1)	30320.0925(−51)	30317.1797(12)	29971.8528(9)	29969.3237(−32)
14	30643.0653(−13)	30639.2491(42)	30249.1216(19)	30245.7679(−26)	29877.6169(−18)	29874.6881(10)
15	30587.1932[b]	30582.9114(−76)	30171.7503(−7)	30167.9445(−14)	29777.8171(−35)	29774.4527(−23)
16	30523.6563(5)	30518.8364(7)	30087.6419(6)	30083.3551(4)	29672.2259[b]	29668.3483[b]
17	30451.8445(−63)	30446.4892(−37)	29996.3877(43)	29991.5895(−11)	29560.3908(−55)	29556.0859(34)
18	—	—	29897.4962(−75)	29892.1849(50)	29442.0793(90)	29437.2456(24)
19	—	—	—	—	—	29311.3922(−35)

[a] The numbers in the parentheses give the observed minus calculated line positions (in the units of 10^{-4} cm^{-1}) using the constants of Tables 4 and 5.
[b] Blended and given no weight in the final fit.

Table 2. Vacuum Wave Numbers for the Lines of the 0–1 Band of $c^1\Pi$–$a^1\Delta$ System of NH[a]

J	R_{ee}	R_{ff}	Q_{ef}	Q_{fe}	P_{ee}	P_{ff}
2	27645.1691(11)	27644.9686(6)	27560.4319(76)	27560.3317(75)	27503.8471(85)	27503.8026(−26)
3	27663.1159(−48)	27662.7870(−10)	27550.3881(70)	27550.1873(61)	27465.6301(−75)	27465.5325(−49)
4	27677.4363(−45)	27676.9413(−16)	27536.9241(23)	27536.5992(100)	27424.1864(40)	27423.9878(55)
5	27688.0148(6)	27687.3190(0)	27519.9878(11)	27519.4899(10)	27379.4704(26)	27379.1363(13)
6	27694.7118(14)	27693.7850(−13)	27499.4976(−26)	27498.8088(35)	27331.4691(−38)	27330.9779(31)
7	27697.3776(−38)	27696.1979(6)	27475.3649(−52)	27474.4467(1)	27280.1646(42)	27279.4589(−60)
8	27695.8626(24)	27694.3768(−88)	27447.4885(25)	27446.3040(9)	27225.4686(−73)	27224.5483(−29)
9	27689.9581(−10)	27688.1577(−66)	27415.7186(3)	27414.2469(12)	27167.3460(0)	27166.1613(1)
10	27679.4655(−17)	27677.3252(22)	27379.9153(−3)	27378.1207(−31)	27105.6775(−2)	27104.2017(−4)
11	27664.1453(−20)	27661.6289(38)	27339.9023(−5)	27337.7678(49)	27040.3659(104)	27038.5632(39)
12	27643.7369(46)	27640.8103(61)	27295.4811(34)	27292.9557(−60)	26971.2455(63)	26969.0969(37)
13	27617.9362[b]	27614.5595(7)	27246.4077(6)	27243.4799(−75)	26898.1628(19)	26895.6323(−42)
14	27586.3704(23)	27582.5545(74)	27192.4077[b]	27189.0714(−6)	26820.9120(−83)	26817.9885(−8)
15	27548.6821(−46)	27544.3773(−25)	27133.2066(−51)	27129.4052(−4)	26739.2775(−29)	26735.9005[b]
16	27504.4440[b]	–	27068.4279[b]	27064.1241(−55)	26652.9625(9)	–
17	–	–	26997.6321(89)	26992.8287(−1)	–	–
18	–	–	26920.3406(−62)	26915.0444(22)	–	–

[a] The numbers in the parentheses give the observed minus calculated line positions (in the units of 10^{-4} cm^{-1}) using the constants of Tables 4 and 5.
[b] Blended and given no weight in the final fit.

Table 3. Vacuum Wave Numbers for the Lines of the 1–0 Band of the $c^1\Pi$–$a^1\Delta$ System of NH[a]

J	R_{ee}	R_{ff}	Q_{ef}	Q_{fe}	P_{ee}	P_{ff}
2	32933.9289[b]	–	32856.9688[b]	32856.8552[b]	32805.5505[b]	32805.5078[b]
3	32937.7208[b]	–	32835.4104[b]	32835.2101[b]	32758.4714[b]	32758.3676[b]
4	32933.9289[b]	32933.4348(−39)	32806.5807(−30)	32806.2411(59)	32704.2790(−70)	32704.0824(66)
5	32922.4557(61)	32921.7359(106)	32770.3363(21)	32769.8138(−6)	32642.9596(−2)	32642.6238(130)
6	32902.9902(57)	32902.0199(−27)	32726.5410(16)	32725.8154(−1)	32574.4156(−88)	32573.8968(−74)
7	32875.3066(−49)	32874.0819(45)	32675.0310(45)	32674.0674(19)	32498.5855(33)	32497.8540(−36)
8	32839.1225(−87)	32837.5888(17)	32615.6015[b]	32614.3471(−23)	32415.3056(70)	32414.3315(−47)
9	32794.0865(5)	32792.1955(64)	32547.9435(−12)	32546.4051(23)	32324.3940(−40)	32323.1665(−35)
10	32739.7392(−69)	32737.4304[b]	32471.7990(55)	32469.8934(−64)	32225.6519(−37)	[c]
11	–	–	32386.7325(−26)	32384.4330(−68)	32118.7862(−13)	32116.8888(−3)
12	–	–	–	–	32003.4430(73)	32001.1370(34)

[a] The numbers in the parentheses give the observed minus calculated line positions (in the units of 10^{-4} cm^{-1}) using the constants of Tables 4 and 5.
[b] Blended and given no weight in the final fit.
[c] Overlapped by a line of the A–X system.

ANALYSIS AND DISCUSSION

The rotational constants for the $c\,^1\Pi$ and $a\,^1\Delta$ states were determined from a nonlinear least-squares fit of the data in Tables 1–3. All three vibrational bands were simultaneously fitted. The rotational energy expressions for these two states are defined as follows:

(for the $^1\Pi$ state)

$$F_v(J) = B_v[J(J+1)-1] - D_v[J(J+1)-1]^2 + H_v[J(J+1)-1]^3 + L_v[J(J+1)-1]^4 \pm \tfrac{1}{2}\{q_v + q_{Dv}J(J+1) + q_{Hv}[J(J+1]^2\}J(J+1),$$

(for the $^1\Delta$ state)

$$F_v(J) = B_v[J(J+1)-4] - D_v[J(J+1)-4]^2 + H_v[J(J+1)-4]^3 + L_v[J(J+1)-4]^4 \pm \tfrac{1}{2}q_v[J(J+1)]^2.$$

In these equations the upper (lower) signs correspond to the e (f) parity [25] components and the constants B, D, H, and L have their usual spectroscopic meaning. The lines of the fundamental vibration–rotation band of the $a\,^1\Delta$ state reported by Hall *et al.*[18] were included in our fits so we could derive more-accurate spectroscopic constants. The data of Hall *et al.*[18] included R-branch lines up to $J'' = 34$ but only two Q-branch lines and no P-branch lines. The rotational constants obtained in the final fit are given in Tables 4 and 5.

It was found that the lambda-doubling constants, q, of the two vibrational levels of the $a\,^1\Delta$ state have appreciable magnitude. Lambda-doubling parameters for $^1\Delta$ states are rarely determined because they are so small. Recently Ubachs *et al.*[11] found q to be −4.82(31) kHz, in excellent agreement with our value of −4.86(69) kHz for $v = 0$ of $a\,^1\Delta$. There is also good agreement between our lambda-doubling parameters and those of Ubachs *et al.*[11] (except for q_H) for the $c\,^1\Pi$ state. However, our rotational constants differ somewhat from those of Ubachs *et al.*[11] For example, our B_0 is 14.15158(10) for the $c\,^1\Pi$ state, while Ubachs *et al.* obtained 14.14203(22). Our B_0 for the $a\,^1\Delta$ state is in excellent agreement with the more accurate value determined by Leopold *et al.*[19] in a far-infrared laser magnetic resonance experiment.

Our value of $\Delta G''_{1/2}$ for $a\,^1\Delta$ is 3182.7879(16), compared with the value of Ramsay and Sarre[10] of 3182.758(35) cm^{-1} and with that of Hall *et al.*[18] of 3182.7768(37). For $\Delta G'_{1/2}$ our value is 2121.4557(69), compared with that of Graham and Lew,[12] 2122.54 cm^{-1}.

Table 4. Rotational Constants (in cm^{-1}) for the $a\,^1\Delta$ State of NH

Constants[a]	$v = 0$	$v = 1$
T_v[b]	0.0	3182.7879(16)
B_v	16.432551(76)	15.814214(87)
$10^4 \times D_v$	16.7309(57)	16.4156(69)
$10^8 \times H_v$	11.54(22)	11.01(24)
$10^{12} \times L_v$	6.0(34)	3.8(30)
$10^7 \times q_v$	−1.62(23)	−1.46(21)

[a] Values in parentheses represent one standard deviation in the last digits.
[b] The singlet–triplet splitting is 12 688.39(10) for $a\,^1\Delta$ ($v = 0$, $J = 2$)–$X\,^3\Sigma^-$ ($v = 0$, $J = 1$, $N = 0$) obtained from the line positions of Tables 1–3 and Refs. 14 and 15.

Table 5. Rotational Constants (in cm^{-1}) for the $c\,^1\Pi$ State of NH

Constants[a]	$v = 0$	$v = 1$
T_v[b]	30704.0818(16)	32825.5375(67)
B_v	14.15158(10)	12.86063(66)
$10^4 \times D_v$	22.462(11)	27.22(19)
$10^8 \times H_v$	−5.89(47)	−52.5(20)
$10^9 \times L_v$	−0.2814(73)	−2.02(71)
$10^3 \times q_v$	16.711(38)	17.67(23)
$10^6 \times q_{Dv}$	−3.92(38)	−14.0(53)
$10^8 \times q_{Hv}$	0.216(88)	9.1(29)

[a] Values in parentheses represent one standard deviation in the last digits.
[b] Measured relative to $a\,^1\Delta$ ($v = 0$).

CONCLUSION

The 0–0, 1–0, and 0–1 bands of the $c\,^1\Pi$–$a\,^1\Delta$ transition of NH were observed by high-resolution Fourier-transform emission spectroscopy. Improved molecular constants were extracted, including the determination of the lambda-doubling parameters for $v = 0$ and $v = 1$ levels of the $a\,^1\Delta$ state.

ACKNOWLEDGMENTS

We are grateful for the expert technical assistance of Rob Hubbard in acquiring the NH spectrum. We thank Jim Brault for the helium spectra employed to calibrate our data and his interest in this work. This work was supported by funding from the U.S. Office of Naval Research.

REFERENCES AND NOTES

1. W. R. Anderson, L. J. Decker, and A. J. Kotlar, Combust. Flame **48,** 179 (1982); M. S. Chou, A. M. Dean, and D. Stern, J. Chem. Phys. **76,** 5334 (1982); J. A. Miller, M. C. Branch, and R. J. Kee, Combust. Flame **43,** 81 (1981).
2. J. L. Schmitt, Pub. Astron. Soc. Pac. **81,** 657 (1969); R. W. Shaw, Astrophys. J. **83,** 225 (1936); D. L. Lambert, J. A. Brown, K. A. Hinkle, and H. R. Johnson, Astrophys. J. **284,** 223 (1984).
3. C. R. Brazier, R. S. Ram, and P. F. Bernath, J. Mol. Spectrosc. (to be published).
4. J. M. Eder, Denkschr. Wien Akad. **60,** 1 (1893).
5. G. Nakamura and T. Shidei, Jpn. J. Phys. **10,** 5 (1935).
6. G. H. Dieke and R. W. Blue, Phys. Rev. **45,** 395 (1934).
7. R. W. B. Pearse, Proc. R. Soc. London Ser. A **143,** 112 (1933).
8. H. Hanson, I. Kopp, M. Kronekvist, and N. Åslund, Ark. Fys. **30,** 1 (1964).
9. W. Y. Cheung, B. Gelernt, and T. Carrington, Chem. Phys. Lett. **66,** 287 (1979).
10. D. A. Ramsay and P. J. Sarre, J. Mol. Spectrosc. **93,** 445 (1982).
11. W. Ubachs, G. Meyer, J. J. ter Meulen, and A. Dymanus, J. Mol. Spectrosc. **115,** 88 (1986).
12. W. R. M. Graham and H. Lew, Can. J. Phys. **56,** 85 (1978).
13. R. W. Lunt, R. W. B. Pearse and E. C. W. Smith, Proc. R. Soc. London Ser. A **155,** 173 (1936); F. L. Whittaker, Proc. Phys. Soc. London **90,** 535 (1967); G. Krishnamurty and N. A. Narasimham, J. Mol. Spectrosc. **29,** 410 (1969).
14. R. W. Lunt, R. W. B. Pearse and E. C. W. Smith, Proc. R. Soc. London Ser. A **151,** 602 (1935); F. L. Whittaker, J. Phys. B **1,** 977 (1968).
15. J. Masanet, A. Gilles, and C. Vermeil, J. Photochem. **3,** 417 (1974); Chem. Phys. Lett. **25,** 346 (1974).
16. D. Cossart, J. Chem. Phys. (Paris) **76,** 1045 (1979).
17. F. Rohrer and F. Stuhl, Chem. Phys. Lett. **111,** 234 (1984).

18. J. L. Hall, H. Adams, J. V. V. Kasper, R. F. Curl, and F. K. Tittel, J. Opt. Soc. Am. B **2**, 781 (1985).
19. K. R. Leopold, K. M. Evenson, and J. M. Brown, J. Chem. Phys. **85**, 324 (1986).
20. U. Blumenstein, F. Rohrer, and F. Stuhl, Chem. Phys. Lett. **107**, 347 (1984); A. Hofzumahaus and F. Stuhl, J. Chem. Phys. **82**, 3152, 5519 (1985); H. K. Haak and F. Stuhl, J. Phys. Chem. **88**, 2201, 3627 (1984).
21. I. Tokue and Y. Ito, Chem. Phys. **52**, 47 (1980); **79**, 383 (1983); **89**, 51 (1984); J. Phys. Chem. **88**, 6250 (1984).
22. W. H. Smith, J. Brzozowski, and P. Erman, J. Chem. Phys. **64**, 4628 (1976).
23. F. Alberti and A. E. Douglas, Chem. Phys. **34**, 399 (1978).
24. The National Solar Observatory is operated by the Association of Universities for Research in Astronomy, Inc., under contract with the National Science Foundation.
25. J. M. Brown, J. T. Hougen, K. P. Huber, J. W. C. Johns, I. Kopp, H. Lefebvre-Brion, A. J. Merer, D. A. Ramsay, J. Rostas, and R. N. Zare, J. Mol. Spectrosc. **55**, 500 (1975).